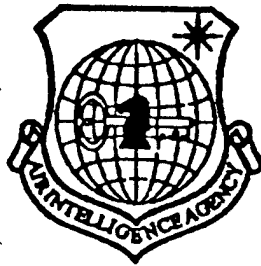


# NATIONAL AIR INTELLIGENCE CENTER



RESEARCH ON GYRO ACCELEROMETER OUTPUT DEVICE

by

Xu Changzhi, Wang Wei and Zhao Caifan

DTIC QUALITY INSPECTED &



Approved for public release:  
distribution unlimited

19970206 026

**HUMAN TRANSLATION**

NAIC-ID(RS)T-0306-96                      7 October 1996

MICROFICHE NR:

RESEARCH ON GYRO ACCELEROMETER OUTPUT DEVICE

By: Xu Changzhi, Wang Wei and Zhao Caifan

English pages: 11

Source: Cama, China Astronautics and Missilery Abstracts,  
Vol. 3, Nr. 1, 1996 (Yuhang Xuebao Journal of Astro-  
nautics, Vol. 16, Nr. 4, October 1995); pp. 70-75

Country of origin: China

Translated by: Leo Kanner Associates  
F33657-88-D-2188

Requester: NAIC/TASC/Richard A. Peden, Jr.

Approved for public release: distribution unlimited.

THIS TRANSLATION IS A RENDITION OF THE ORIGINAL FOREIGN TEXT WITHOUT ANY ANALYTICAL OR EDITORIAL COMMENT STATEMENTS OR THEORIES ADVOCATED OR IMPLIED ARE THOSE OF THE SOURCE AND DO NOT NECESSARILY REFLECT THE POSITION OR OPINION OF THE NATIONAL AIR INTELLIGENCE CENTER.	PREPARED BY:  TRANSLATION SERVICES NATIONAL AIR INTELLIGENCE CENTER WPAFB, OHIO
--	---

**GRAPHICS DISCLAIMER**

All figures, graphics, tables, equations, etc. merged into this translation were extracted from the best quality copy available.

# Research on Gyro Accelerometer Output Device

Xu Changzhi, Wang Wei and Zhao Caifan

(Beijing Control Device Research Institute, Beijing, 100854)

**Abstract:** To design a new gyro accelerometer output device, this paper advances a miniaturized high-speed and high-precision dynamic goniometric system plan and discusses the engineering realization of this plan. In fact, this goniometric system has already been successfully applied to a static pressure liquid-floated gyro accelerometer.

**Key Words:** Accelerometer, inertial navigation, signal detection

## 1. Introduction

The gyro accelerometer used to measure the time-integral volume of the carrier's apparent acceleration in a given direction, i.e. the carrier's apparent acceleration, is supposed to possess high precision, a wide measurement range and high reliability. As a signal detection system of the gyro accelerometer, the output device must have the capability of accurately measuring the distance of the corner of the accelerometer outer ring relative to the shell, and delivering it to the guidance computer in the form of digital pulses. Essentially, it is a high precision pulse-output dynamic goniometric system which should meet the index requirements in the following four aspects:

- (1) Resolution and pulse equivalent;
- (2) Number of pulses required for one round of precession of the accelerometer;

(3) Excellent dynamic tracking performance and jamming-proof capability and

(4) Small volume of element devices.

Technically, the variable magnetic resistance phase locking multiple frequency goniometric system plan presented in this paper is a digital output of open-loop increment type, in which the circuit is simple, the reliability, precision and tracking speed are easy to increase, the pulse equivalent requirement is easy to meet, and the device conditions required are rather well developed.

## 2. Principle of the Goniometric System

### 2.1 Operation Mode of the Goniometric Sensor

Among other things,

$\Delta\omega$ ---Initiation power supply frequency difference

$\omega_0$ ---Initiation power supply standard frequency

$\alpha_0$ ---Rotor electric corner

$\Delta\phi$ ---Phase-shift error

$\varepsilon$ ---Relative value of amplitude value error

$\omega_n$ --- $\alpha_0 = P \cdot \theta(t)$  ( $P$  is the polar logarithm;  $\theta(t)$  is a mechanical corner)

$\omega$ ---Initiation frequency

$\Delta\phi_2$ ---Quadrature phase error of two phase initiation power supply

$\varepsilon_2$ ---Relative value of two phase initiation power supply amplitude value error

The angular module transformation of the magnetic resistance multipole rotating transformer, adopted in this paper, is a phase discrimination form. Table 1 shows the dynamic and static errors in three operation modes (the ratio system is simplified as 1).

At the same time, in consideration of the size and technological factors, this paper selects the two phase initiation and single phase output mode, whose static error is basically caused by power supply error, while the dynamic error is a small bivalent amount.

Table 1. Error Analysis in Three Operation Modes ("error" is the electric angular error, the unit is radian)

1 方式 2 误差		3 条件		
		4 一相激磁两相输出	5 两相激磁一相输出	6 两相激磁两相输出
7 静态	8 电源误差		$\frac{1}{2}\Delta\varphi_2 + \frac{1}{2}\Delta\varphi_2\cos 2\alpha_D$ $-\frac{1}{2}\varepsilon_2\sin X_D$	$\frac{1}{2}\Delta\varphi_2$
	9 幅相变换误差	$\frac{1}{2}\Delta\varphi - \frac{1}{2}\Delta\varphi\cos 2X_D$ $-\frac{1}{2}\varepsilon\sin 2\alpha_n$	13 无	13 无
10 动态	11 电源理想	$-\frac{\omega n}{2\omega} [1 - \cos(2X_n - \frac{\omega n}{2\omega})]$	13 无	13 无
	12 电源不理想		$\frac{\omega n}{2\omega} (\Delta\varphi - \varepsilon\sin 2\alpha_n - \Delta\varphi\cos 2\alpha_n)$	$\frac{\omega n \Delta\varphi}{2\omega}$

Key: (1) Mode; (2) Error; (3) Condition; (4) One phase initiation and two phase output; (5) Two phase initiation and one phase output; (6) Two phase initiation and two phase output; (7) Static state; (8) Power supply error; (9) Phase and amplitude transformation error; (10) Dynamic state; (11) Ideal power supply (12) Non-ideal power supply; (13) None

## 2.2 Working Principle of the Goniometric System

In accordance with the operation mode of the sensor, a phase

locking multiple frequency geometric system plan was proposed as shown in Fig. 1.

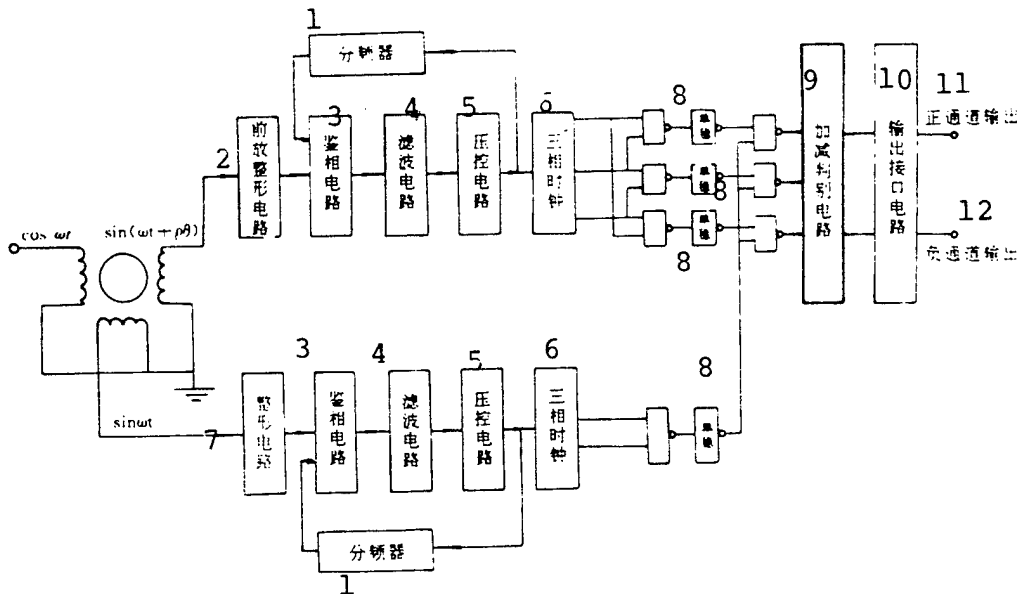


Fig. 1. A Variable Magnetic Resistance Phase Locking Multiple Frequency Goniometric System

Key: (1) Frequency divider; (2) Prepositioned reshaping circuit; (3) Phase discrimination circuit; (4) Filtering circuit; (5) Pressure control circuit; (6) Three-phase clock; (7) Reshaping circuit; (8) Monostability; (9) Add-subtract discrimination circuit; (10) Output interface circuit; (11) Positive channel output; (12) Negative channel output

This system adopts the two-phase initiation cross power supply to make the initiation windings of the sensor cross in space and therefore, the voltage of the output winding is:

$$u_1 = \sin(\omega t + P \cdot \theta) \tag{1}$$

where  $P, \theta$  are equal to those marked in the Table;  $\omega$  is the initiation angular frequency.

The  $u_1$  signal, through amplification and reshaping, is subject to phase amplification by the square wave phase locking signal frequency ring circuit with its output square wave as:

$$u_2 = S[N\omega t + NP\theta] \quad (2)$$

where  $N$  is the number of multiple frequencies.

Similarly, with reshaping and frequency multiplication of the reference signal, the following is derived:

$$u_3 = S[N\omega t] \quad (3)$$

To separate the changed portion of the output signal from the pressure control oscillator, the add-subtract discrimination circuit of three-phase clock type was employed to make a phase sequence comparison between  $u_2$  and  $u_3$  and single out the useful signal, which is quantized and output in digital form with the resolution as:

$$\delta = 2 \times 360 \times 60 / (P \cdot \theta) \text{ (angular resolution)} \quad (4)$$

### 3. Engineering Realization of Phase Locking Multiple Frequency Goniometric System

#### 3.1 Design and Realization of Goniometric System

##### (1) Phase Locking Multiple Frequency Ring Circuit

This is a closed-loop phase synchronous control ring circuit, which plays the role of phase amplification and filtering. Its tracking characteristics determine the goniometric tracking characteristics. According to the

resolution requirement of the system, the number of multiple frequencies of the ring circuit  $N$  can be determined. Fig. 2 indicates the phase model of the ring circuit in the linear tracking state. When the ring circuit is locked, the feedback phase signal  $\theta_b(S)$  tracks the change in input phase signal  $\theta_{in}(S)$ , and the output phase  $\theta_o(S)$  is  $N$  times the  $\theta_{in}(S)$ .

To ensure float tracking of  $\theta_o(S)$  over  $\theta_{in}(S)$  and suppress the input interference  $\theta_{fin}(S)$ , the phase discriminator sampling noise  $\theta_{fd}(S)$  and the pressure control oscillator noise  $\theta_{fco}(S)$  so that the system can function in normal conditions, this paper explored, based on the design of the Robustness circuit filter in a broad sense, a simple and effective correction network as shown in Fig. 3. Its transfer function  $F(S)$  is :

$$F(S) = \frac{(R_1 C_1 S + 1) \left( \frac{R_2 C_4}{2} S + 1 \right)}{R_1 S (R_2^2 C_4^2 S^2 + 2 R_2 C_4 S + 1) (R_1 C_1 S + C_1 + C_2) \left( \frac{R_2 C_3}{2} S + 1 \right)} \quad (5)$$

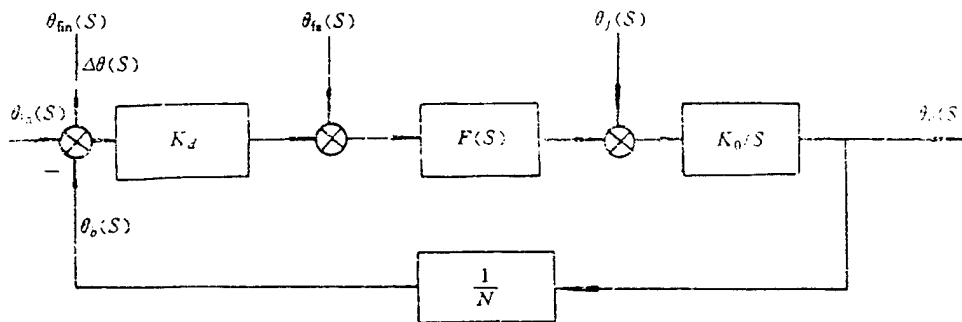


Fig. 2. Phase Model of Phase Locking Multiple Frequency Ring Circuit

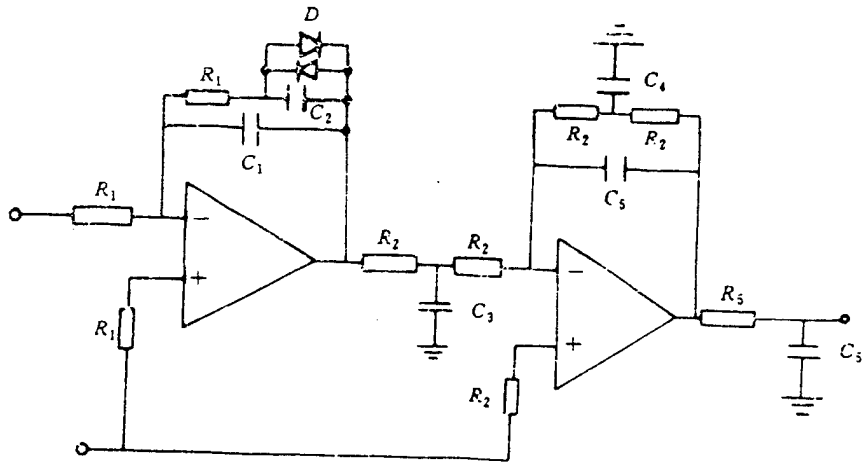


Fig. 3 Filtering Correction Network Circuit

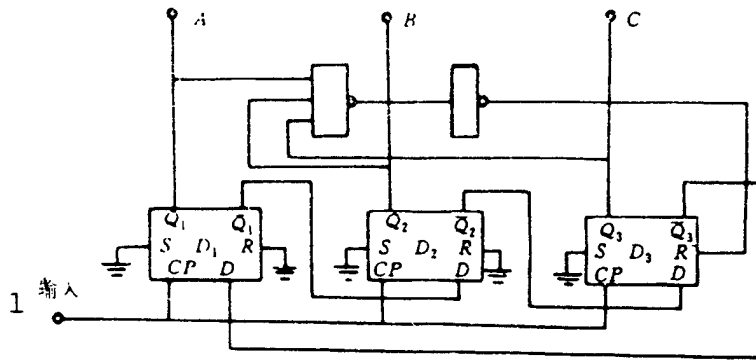


Fig. 4. Three-Phase Clock Circuit

Key: (1) Input

## (2) Three-Phase Clock and Add-subtract Discrimination Circuit

The three-phase clock circuit converts the input periodical square wave signal into a square wave signal with a  $120^\circ$  difference among three phases. Its circuit is shown in Fig. 4.

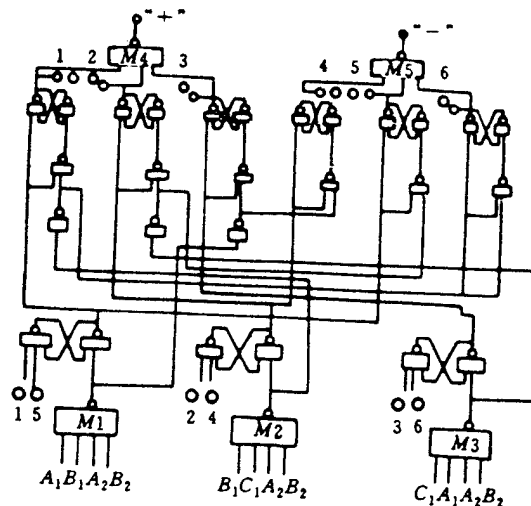


Fig. 5 Add-subtract Discrimination Circuit

The add-subtract discrimination circuit is shown in Fig. 5. Through a comparison and discrimination between the three-phase sequence pulses  $V_{A1}$ ,  $V_{B1}$ ,  $V_{C1}$  and two of the three standard phase pulses of the reference signal circuit  $V_{A2}$ ,  $V_{B2}$ , this circuit can identify the phase difference and direction of the two circuit signals and output them in positive and negative pulses. When the sensor rotor rotates positively, the clock signal of the measurement signal circuit shifts its phase to the left relative to the reference circuit signal. In this case, the low potential appears in NAND gate order:  $M_1 \rightarrow M_2 \rightarrow M_3 \rightarrow M_1 \dots$ , and through the rear pole circuit discrimination,  $M_4$  outputs pulses while  $M_5$  does not. On the contrary, when the sensor rotates in reverse, only  $M_5$

outputs pulses but  $M_4$  does not. In reality, however,  $M_1$ ,  $M_2$  and  $M_3$  cannot generate low potential simultaneously.

Accordingly, governed by the Robust adjustment principle, a damping vibration-reducing circuit composed of NAND gate and monostability was added to the input terminal of  $M_1$ ,  $M_2$  and  $M_3$ . This increased the system capability of suppressing the high-frequency noise and effectively decreased the interference pulses generated by VCO noise as shown in Fig. 6. In addition, an output reshaping circuit was designed to match the computer input.

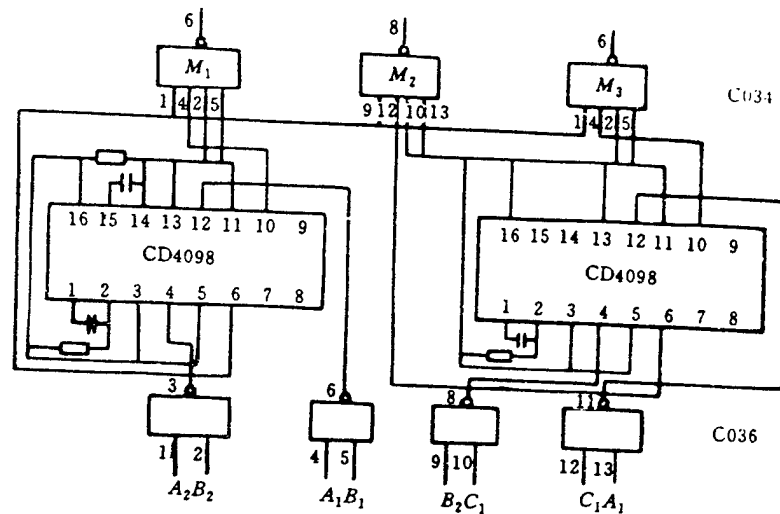


Fig. 6 Damping Vibration-reducing Circuit

### 3.2 Goniometric System Error Analysis

Basically, the errors of this goniometric system include the sensor errors, tracking errors of the phase locking ring circuit and circuit errors.

(1) The sensor errors mainly involve angular module transformation errors, technological errors and adjustment

uncertainty errors, which are expressed in the form of function errors and zero-place repetition errors of the sensor output signals. When the two-phase initiation power supply generates relative amplitude value errors and quadrature phase errors, they may cause angular module errors. Its static error  $\Delta\phi_j$  and dynamic error  $\Delta\phi_{do}$  can be calculated using the equation in Table 1. The technological and adjustment errors are determined by factors including throat graduation errors; concentricity, ellipticity, winding accuracy and installation precision. This error can be controlled within the required precision through technological improvement and proper compensation.

(2) The tracking error of the phase locking ring circuit is determined by the ring circuit error transfer function  $G_e(S)$ . Once the form of the measured signal  $\theta_{in}(t)$  is known, the phase locking tracking error can be calculated based on the actual working time  $t$ . This error in our system is 2 orders of magnitude smaller than the sensor error.

(3) The circuit errors consist of the prepositioned amplified static error, and the add-subtract discrimination circuit error. The former can be calculated through Eq. (6). These errors in our system are one order of magnitude smaller than the sensor error.

$$\Delta\alpha_{qj} = \arcsin \frac{\Delta U}{U_m} \quad (6)$$

where  $U_m$  is the maximum output voltage,  $\Delta U$  is the noise voltage and  $\Delta\alpha_{qj}$  is the prepositioned amplified static error.

The add-subtract discrimination circuit requires a two-period phase difference, i.e.  $4\pi$  phase difference between the pressure control signals of circuits I and II for one pulse output, which is equivalent to the resolution of the system.

#### 4. Conclusions

The foregoing output device, mounted on the outer ring of the static pressure liquid-floated gyro accelerometer, in accordance with instrument specifications, underwent various environmental experiments, such as fixed frequency sinusoidal vibration, sinusoidal scan vibration, random vibration, impact, centrifuging and high and low temperature experiments. As a result, it realized rather high goniometric precision and dynamic goniometric speed. The output device system plan and its engineering design, proposed and realized in this paper, showed the desired performance.

#### References

1. Shao Wenzheng, Xu Changzhi et al., A New Output Device of Gyro Accelerometer, Inertial Guidance and Instruments, 1987.
2. Lu Yongping et al., Induction Synchronizer and Its System, National Defense Industry Press, 1986.

This paper was received on August 17, 1993.